Quantum confinement in Si- and Ge-capped nanocrystallites

L. E. Ramos, J. Furthmüller, and F. Bechstedt
Institut für Festkörpertheorie und -optik, Friedrich-Schiller-Universität Jena, 07743 Jena, Germany
(Received 11 January 2005; revised manuscript received 23 May 2005; published 22 July 2005)

We present an *ab initio* plane-wave-pseudopotential investigation of Si- (Ge-)capped Ge (Si) nanocrystallites. The effects of capping Si and Ge nanocrystallites on the electron-hole pair excitation energies, optical absorption spectra, localization of the highest-occupied and lowest-unoccupied molecular orbitals, Stokes shifts, and radiative lifetimes are analyzed. The bond lengths and the localization of electrons and holes in the Si- (Ge-)capped nanocrystallites are similar to those found in the analogous Si/Ge heterostructures. Due to the changes in the quantum confinement properties caused by the capping, there are significant differences in the electronic and optical properties of Ge-capped Si nanocrystallites and Si-capped Ge nanocrystallites.

DOI: 10.1103/PhysRevB.72.045351 PACS number(s): 61.46.+w, 68.65.Hb, 73.22.−f, 78.67.Bf

I. INTRODUCTION

The electrical and mechanical properties resulting from the combination of group-IV compounds such as Si and Ge indicate that their heterostructures and nanostructures are very promising materials in device technology.[1] Although Ge is more expensive than Si, it is comparatively cheaper and more compatible with Si technology than the low-gap III-V and II-VI semiconductors.[2] Direct applications of the SiGe technology comprehend high-frequency transistors,[1,3] infrared photodetectors and photodiodes,[4] and solar cells.[5] The performance of SiGe-based photodetectors and solar cells can be enhanced by a gap reduction and the optical absorption at long wavelengths may become more efficient due to increase of Ge content.[5] Besides new features in the electronic properties, SiGe-based nanocrystallites (NCs) can provide different quantum confinement for carriers and charge-storage mechanisms, the latter being useful for low-power memory devices.[6,7]

Light emission from SiGe devices is more difficult to obtain than detection, due to the indirect-gap character of Si and Ge bulk. However, due to quantum confinement effects, luminescence can be observed in porous Si and porous Ge as well as Si and Ge NCs.[8–13] In recent years, considerable progress has been made by employing Si and Ge nanostructures and optical gain has been reported.[14] For light-emitting devices an efficient radiative recombination of holes and electrons is desirable, whereas for solar cells and photodetectors it is important that the absorbed energy is converted into electrical current. Quantum confinement can be used both to enhance and to prevent radiative recombination of holes and electrons by localizing these carriers in different spatial regions. For instance, in type-II Si/Ge heterostructures, the holes are mainly localized in the Ge layers, whereas the electrons are localized in the Si layers.[15,16]

The high lattice mismatch between Si and Ge crystals and the high miscibility of SiGe alloys in principle represent an obstacle for the growth of sharp Si/Ge interfaces, heterostructures, and nanostructures.[17–19] The growth of Ge on Si surfaces usually leads to island formation after the deposition of more than three monolayers of Ge,[19] whereas the growth of Si on Ge surfaces favors the Si indiffusion and the intermixing of species.[20] Recently, the properties of nanometer-sized group-IV NCs with capping-shell structure have been analyzed and studied intensively.[21–27] Although Si-capped Ge NCs are the most common structures assembled,[21–26] structures such as domes whose cores are richer in Si than in Ge have been observed.[27] With the progress of growth techniques or the advent of new methods, one can envisage the synthesis of both Si-capped Ge NCs and Ge-capped Si NCs. The idea of modifying carrier confinement in NCs by means of capping shells has been already studied in II-VI NCs with a core-shell structure.[28–30] Oxidized Si NCs share the same core-shell structure of the II-VI NCs, though their shells are composed of amorphous Si oxide.[31] The confinement of holes and electrons in different regions of the NC has important consequences for the electronic and the optical properties such as luminescence, photostability, and electron accessibility.[29]

Although there are many theoretical investigations on quantum confinement and optical and electronic properties of Si and Ge NCs,[32–39] only few of them take into account systems where Si-Ge bonds and Si/Ge interfaces are present.[37,40–42] The quantum confinement properties of Si- (Ge-)capped Ge (Si) NCs and the effect of an additional Si/Ge potential barrier have not been investigated.

In this paper, we apply *ab initio* plane-wave-pseudopotential calculations to study ideal Si- (Ge-)capped Ge (Si) NCs with a core-shell structure. The methods and the models applied for the NCs are described in Sec. II. Results concerning the structure, electronic and optical properties, Stokes shifts, and radiative lifetimes are discussed in Sec. III. In Sec. IV we sum up the conclusions.

II. METHODS

We apply density-functional theory (DFT) and local-density approximation (LDA) implemented in the VASP code.[43,44] The interaction of the valence electrons with the nuclei is modeled by means of pseudopotentials generated in accordance with the projector-augmented wave (PAW) method, which are reliable to calculate optical matrix elements among other properties.[45] When using PAW pseudopotentials, an energy cutoff of 15 Ry for the plane waves is sufficient to achieve a good convergence of total energies

 ©2005 The American Physical Society

(less than 0.03% of variation with further increase of the cutoff) and atomic forces (less than 30 meV/Å). This low-energy cutoff allows us to treat NCs with sizes comparable to the ones observed in experiments. Calculations for Si and Ge bulk in the diamond structure lead to optimized bond lengths of 2.34 Å and 2.44 Å, respectively.

The NCs we study have a shell-like structure. Starting from a central Si atom and assuming tetrahedral coordination, the NCs are constructed by adding the neighboring atoms shell by shell. The surfaces of all NCs considered are faceted and the dangling bonds are always passivated with hydrogen atoms. Although the passivation with hydrogen can be considered as a kind of capping for the NCs, in the following "capped NCs" refers to those with outermost shells containing group-IV atoms different from the ones of their core. We consider free-standing NCs with 41 Si (Ge) atoms (four shells) in the core and capped with a maximum of three Ge (Si) atom shells. NCs with 17 Si (Ge) atoms in the core (three shells) and two capping Ge (Si) shells are also studied for purposes of comparison. The calculations are performed using simple-cubic supercells, where more than 15 Å of vacuum separates the facets of the free-standing structures from the facets of their supercell images, which prevents a strong NC-NC interaction. Ge-capped Si NCs with one, two, and three capping shells contain, respectively, 191 ($Si_{41}Ge_{42}H_{108}$), 295 ($Si_{41}Ge_{106}H_{148}$), and 459 ($Si_{41}Ge_{198}H_{220}$) atoms in the supercell. To simplify the description of the NCs, in the following we denote them according to the number of atom shells in their core and in their capping shells. Therefore, Si4Ge1 means four Si atom shells in the core and one Ge capping shell, Ge3Si2 means three Ge atom shells in the core and two Ge capping shells, and so on. In order to achieve a total-energy minimum and negligible interatomic forces, we perform the ionic relaxation for all NCs under constrained T_d point symmetry, which resembles the symmetry of bulk Si and Ge. For comparison we also perform calculations without symmetry constraint, which are important to study excited states. After the relaxation, the capped Si (Ge) NCs have average diameters varying from 15 to 23 Å, which are sizes comparable to those of the capped II-VI NCs.[28–30] Two capped NCs structures resulting from the ionic relaxation are shown in Fig. 1. We also study the relaxation of Si-capped Si NCs and Ge-capped Ge NCs containing the same number of atoms as for the capped Si and Ge NCs.

The optical matrix elements are calculated within the framework of the independent-particle approximation, and the optical absorption spectra are identified as the imaginary part of the corresponding dielectric function. The spectra are presented with a Lorentzian broadening of 0.1 eV. Within DFT LDA, the calculated fundamental gaps of bulk Si and bulk Ge are smaller than their respective experimental values. In particular for Ge, the calculated DFT LDA fundamental gap is nearly zero. Due to the quantum confinement in Si and Ge NCs, the DFT LDA gaps are much larger than the ones calculated for Si and Ge bulk, respectively. Even restricted to DFT and the LDA, one can obtain more reliable values for pair excitation energies by applying the Δ self-consistent field method. In the framework of the Δ self-consistent field method,[35] we calculate the lowest electron-

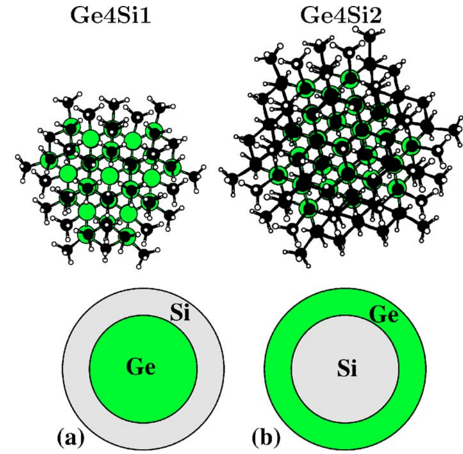

FIG. 1. (Color online) Structure of Si-capped Ge NCs with one (Ge4Si1) and two (Ge4Si2) Si capping shells. The core of the structures contain 41 atoms (four shells). In the lower panels schematic representations of a Si-capped Ge NC (a) and Ge-capped Si NC (b) are shown.

(e-) hole-(h-) pair excitation energies ($E^{e\text{-}h}_{\text{pair}}$) for the NCs containing N electrons by means of total-energy differences $E^{e\text{-}h}_{\text{pair}}=E(N,e+h)-E(N)$. The lowest electron-hole pair excitation energies account for both quasiparticle and excitonic effects. For Si and Ge NCs passivated with hydrogen, it has been verified that the values of $E^{e\text{-}h}_{\text{pair}}$ are very similar to the DFT LDA gaps.[35] By performing the ionic relaxation of the system containing an electron-hole pair, we determine the optimized geometry of this excited electronic state and calculate the Stokes shift by $\Delta_{\text{Stokes}}=[E(N,e+h)-E(N)]-[E^*(N,e+h)-E^*(N)]$, where $E^*(N,e+h)$ and $E^*(N)$ are the total energies of the system in the optimized geometry of the excited state. The influence of the symmetry constraint on the values of the Stokes shift is analyzed by calculating $E^*(N,e+h)$ and $E^*(N)$ also without any symmetry constraint during the ionic relaxation.[46]

The radiative recombination rates $W_{i,j}$ correspond to optical transitions involving unoccupied states $|i\rangle$, with energy equal to or higher than the lowest-unoccupied molecular orbital (LUMO), and occupied states $|j\rangle$, with energy equal to or lower than the highest-occupied molecular orbital (HOMO). The $W_{i,j}$ are calculated from the transition probabilities by[47,48]

$$W_{i,j} = \frac{16\pi^2}{3} n \frac{e^2}{h^2 m^2 c^3} (\varepsilon_i - \varepsilon_j) |\langle i|\mathbf{e}\cdot\mathbf{p}|j\rangle|^2, \tag{1}$$

where $\mathbf{e}$ is the direction of light polarization, $\mathbf{p}$ is the momentum operator, n is the refractive index, and ε_i and ε_j are the energies of the single-particle states $|i\rangle$ and $|j\rangle$, respectively. The radiative lifetime τ corresponds to the inverse of the thermally averaged recombination rate at the absolute temperature T

$$\tau = \frac{\sum_{i,j} \exp[-(\varepsilon_i - \varepsilon_j)/k_B T]}{\sum_{i,j} W_{i,j} \exp[-(\varepsilon_i - \varepsilon_j)/k_B T]}, \tag{2}$$

where k_B is the Boltzmann constant. Since most experiments are carried out at room temperature we set $T=300$ K in Eq.

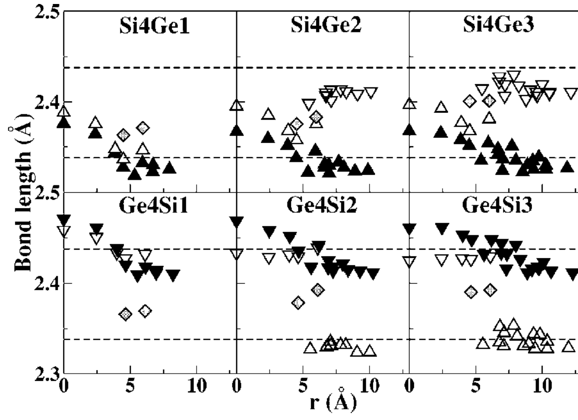

FIG. 2. Si-Si bond lengths (up triangles), Ge-Ge bond lengths (down triangles), and Si-Ge bond lengths (diamonds) versus distance of the atom from the center of the NC for the Ge-capped Si NCs (upper panels) and for the Si-capped Ge NCs (lower panels). The Si-Si bulk bond length (2.34 Å) and the Ge-Ge bulk bond length (2.44 Å) are indicated by the dashed lines. The filled triangles correspond to the Si and Ge NCs passivated with H and with the same number of shells as the capped Si (Ge) NCs in each frame.

(2). This approach does not take into account spin polarization and assumes that the thermalization of the electrons and holes after their injection is more efficient than the radiative recombination.[47,48] As refractive index n, we apply the square root of the dielectric constant obtained by application of the effective-medium theory described in Ref. 38.

III. RESULTS AND DISCUSSION

A. Bonding, structure, and energetic stability

The bond lengths for each atom in the NCs are initially calculated and grouped according to their type, Si-Si, Ge-Ge, and Si-Ge. When one atom has more than one bond of a certain type an average value is calculated. The resulting bond lengths of the capped Si (Ge) NCs and Si (Ge) NCs after ionic relaxation are shown in Fig. 2 versus the distances of the atoms from the center of the NC. As reported in the literature, both Si and Ge NCs passivated with hydrogen exhibit an expansion of the Si-Si or Ge-Ge bond lengths with respect to their bulk value at the center of the NC and a contraction of the same bonds near the surface.[35] For the Ge-capped Si NCs, the Si-Si bonds lengths follow the same trend as for the Si NCs. The Ge-Ge bond lengths in the capping shells are smaller than the one for Ge bulk and tend to have similar values with increasing number of capping shells. On the other hand, for the Si-capped Ge NCs, there is a tendency for both Ge-Ge and Si-Si bond lengths to be slightly smaller than their corresponding bulk values and to vary much less than for the Ge NCs. This occurs in the cores of the Ge NCs and in the capping Si shells as well. The Si-Ge bonds at the interface between the capping shell and the NC core increase with an increasing size of the NC in both Si-capped and Ge-capped structures.

The growth of Si on Ge substrates and the growth of Ge on Si substrates are known to be different.[49] While the growth of Si on Ge is expected to occur in a similar way to the growth of Si on Si surfaces and with high degree of intermixing, the growth of Ge on Si is characterized by the formation of islands after the third Ge monolayer and exhibits practically no intermixing.[18–20] The Si-Si and Ge-Ge bond lengths in the Si-capped Ge NCs indicate a small strain of the bonds which is even lower than the one for Ge NCs. Also the Si-Ge bond lengths increase with the number of capping shells and have similar values in both Si-capped Ge NCs and Ge-capped Si NCs. Although the residual forces in the relaxed NCs are negligible in all cases considered, the increase of the Si-Ge bonds can indicate an accumulation of strain in the capped NCs with increasing number of capping shells. The fact that the Si- (Ge-)capped Ge (Si) NCs are well-ordered core-shell structures gives rise to two defined regions of bond lengths, one at the core and another at the capping shells. Such a behavior for the bond lengths was predicted by means of semiempirical methods by Torre and co-workers for Ge NCs embedded in a Si matrix[40] and is supported by experimental data.[22,23] By applying only thermodynamic considerations, Balasubramanian and co-workers predicted that extremely large Ge NCs could be capped with Si without giving rise to dislocations.[41] In the case of Ge-capped Si NCs, the deviation of the Si-Si and Ge-Ge bond lengths with respect to their bulk values helps to understand the difficulties observed in obtaining a two-dimensional (2D) epitaxial growth of Ge layers on top of Si surfaces. While the capping of NCs modeled in our calculations can be compared to a certain 3D epitaxial growth,[19] the epitaxy experiments usually aim to achieve a 2D growth, the latter changing to a 3D growth in the Stranski-Krastanov mode. From x-ray measurements performed by Woicik and co-workers,[50] the Si-Ge and the Ge-Ge bond lengths at a Si/Ge interface are not expected to be much different from the value measured in a SiGe alloy. According to previous calculations for SiGe NCs, the Si-Si, Si-Ge, and Ge-Ge bond lengths, apart from some variations, do not differ much from the corresponding bulk bond lengths.[37,51] Our findings for Si- (Ge-)capped Ge (Si) NCs agree qualitatively with experiments and also with previous calculations for alloys and Si-Ge structures described above.

To study the energetic stability of the NCs, we calculate their formation energy

$$\Omega(\mathrm{NC}) = E_{\mathrm{tot}}(\mathrm{NC}) - \mu_{\mathrm{Si}}[N_{\mathrm{Si}} - N_{\mathrm{H}}(\theta/4)] - \mu_{\mathrm{SiH}}N_{\mathrm{H}}\theta - \mu_{\mathrm{Ge}}[N_{\mathrm{Ge}} - N_{\mathrm{H}}(1-\theta)/4] - \mu_{\mathrm{GeH}}N_{\mathrm{H}}(1-\theta) \quad (3)$$

for Ge-capped Si NCs ($\theta=0$) and Si-capped Ge NCs ($\theta=1$), where $E_{\mathrm{tot}}(\mathrm{NC})$ is the total energy of the NC, N_X ($X=\mathrm{Si},\mathrm{Ge},\mathrm{H}$) is the number of atoms X, $\mu_{\mathrm{Si}}=-5.93$ eV/atom and $\mu_{\mathrm{Ge}}=-5.17$ eV/atom are the chemical potentials per atom of Si and Ge bulk, respectively, and $\mu_{\mathrm{SiH}}=-4.79$ eV/bond and $\mu_{\mathrm{GeH}}=-4.50$ eV/bond are the Si-H and Ge-H bond energies, obtained from calculations for the molecules SiH_4 and GeH_4. For Si-capped Si NCs and Ge-capped Ge NCs the formation energies are calculated by

$$\Omega(\mathrm{NC}) = E_{\mathrm{tot}}(\mathrm{NC}) - \mu_X[N_X - N_{\mathrm{H}}/4] - \mu_{X\mathrm{H}}N_{\mathrm{H}}, \quad (4)$$

where $X=$Si and Ge respectively. The formation energies Ω calculated by Eqs. (3) and (4) and shown in Fig. 3 corre-

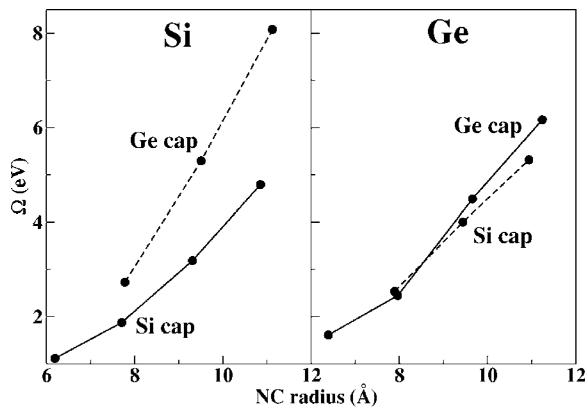

FIG. 3. Formation energies versus radius for NCs with a Si core (left) and for NCs with a Ge core (right). The solid lines indicate Si capping shells (left) and Ge capping shells (right), whereas the dashed lines indicate Ge capping shells (left) and Si capping shells (right).

spond to a specific preparation condition of the NCs, where the energy of the H bonds to Si and Ge are taken into account. They indicate that Ge-capped Si NCs are the least energetically favorable, and are less stable than Si NCs passivated with H with equal total number of atoms. On the other hand, the formation energies of Si-capped Ge NCs are closer to the formation energies of Ge NCs passivated with H. This is in qualitative agreement with what is observed in experiments, where the Si-capped Ge NCs are the most common structures.[21–26]

B. Electronic properties

Given the high miscibility expected between Si and Ge in a system which contains both elements, we first analyze in Fig. 4 the role of the stoichiometry in the electronic properties. Neglecting for a moment the fact that our capped NCs are well-ordered ideal structures, we consider them as possible configurations of SiGe-alloy NCs with a certain Ge molar fraction (x_{Ge}). In Fig. 4, we show the lowest electron-

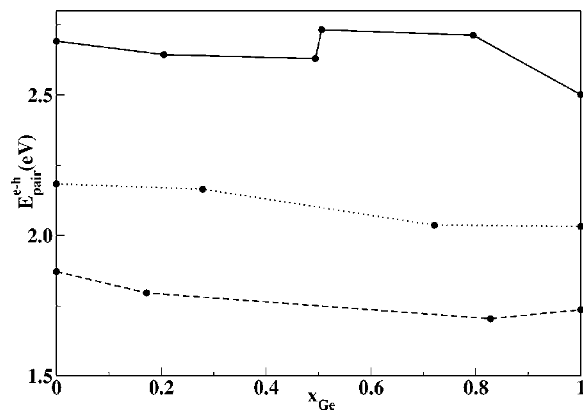

FIG. 4. Electron-hole pair excitation energies versus Ge concentration x_{Ge} in the NC. The curves correspond to NCs with the same total number of shells: five (solid line), six (dotted line), and seven shells (dashed line).

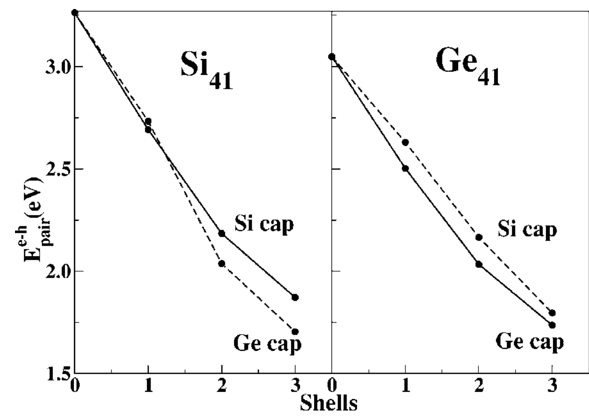

FIG. 5. Electron-hole pair excitation energies versus the number of capping shells for a NC with 41-Si-atom core (left) and for a NC with a 41-Ge-atom core (right). The solid lines indicate the capping with Si atom shells (left) and Ge atom shells (right), whereas the dashed lines indicate the capping with Ge atom shells (left) and Si atom shells (right).

hole-pair excitation energies versus x_{Ge} for relaxed NCs with different total number of shells. For comparison, the electron-hole pair energies for the Si3Ge2 and Ge3Si2 NCs, both with 17 atoms in the core, are shown in the curve corresponding to five atom shells in Fig. 4. The difference between the average radius of a Si NC ($x_{Ge}=0$) and the average radius of a Ge NC ($x_{Ge}=1$) is less than 0.4 Å, for relaxed NCs with equal number of shells. We remark that as for Si and Ge NCs,[35] the plain values of the DFT LDA HOMO-LUMO gaps are different by less than 0.1 eV from the lowest electron-hole pair excitation energies. Those differences are more related to the quantum confinement and composition of the NCs and less related to the passivation of the NCs, since the Si-H and Ge-H bond lengths and bond energies are very similar. As shown in Fig. 4, NCs with the same number of shells or atoms lead to similar electron-hole pair excitation energies. This means that the quantum confinement effects play a more important role than the chemical composition for the values of the pair excitation energies. For a fixed size, the particular arrangement of the Si and Ge atoms in the NCs and their stoichiometry can change the value of electron-pair excitation energies by less than 0.1 eV. The variation of the pair excitation energies versus Ge molar fraction x_{Ge} for NCs with the same number of shells follows the trend predicted for a SiGe alloy.[37] As expected the pair excitation energies for Ge NCs are lower than for Si NCs. The replacement of Si atoms by Ge atoms in the NCs tends to reduce slightly the electron-hole pair excitation energies.

In Fig. 5, we present the same electron-hole pair excitation energies as in Fig. 4 but versus the number of Si (Ge) capping shells for the Ge (Si) NCs with a fixed NC core. The electron-hole pair excitation energies of Si and Ge NCs are smaller for a larger size of the particle, as a result of the reduction of quantum confinement.[35] In addition to this, the large Ge bond lengths in the capping shells tend to lower the carrier confinement. The two types of systems under consideration, Ge-capped Si NCs and Si-capped Ge NCs, exhibit different tendencies with respect to the pure NCs. The addition of Ge capping shells to the Si NC core tends to lower

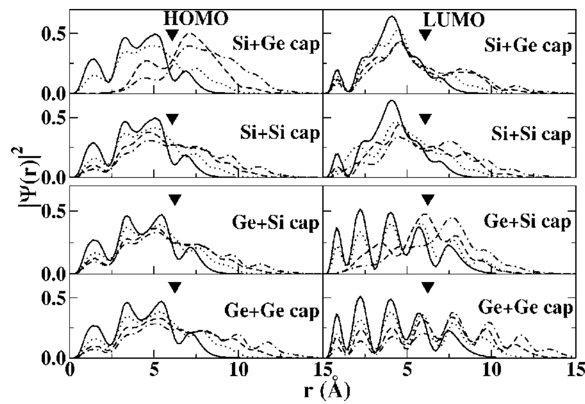

FIG. 6. Radial probability distribution of HOMO (left panels) and LUMO (right panels) versus the distance r from the center of the NC. Starting from the top, the HOMO and LUMO radial distributions are shown for Ge-capped Si NCs, Si NCs, Si-capped Ge NCs, and Ge NCs. For a NC with a 41-atom Si (Ge) core the probability distributions are shown for the case without capping shells (solid lines), one (dotted lines), two (dashed lines), and three (dot-dashed lines) capping shells. The triangles indicate the average radius of the 41-atom NC core.

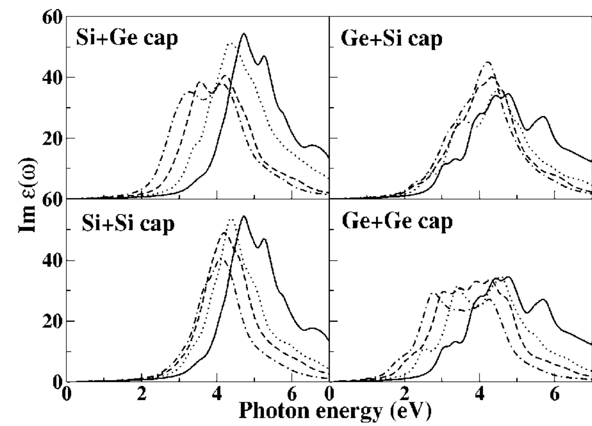

FIG. 7. Optical absorption spectra of NCs with Si core (left panels) and NCs with Ge core (right panels). The upper panels correspond to the capped structures, whereas the lower panels show the spectra of Si and Ge NCs. For a NC with a 41-atom Si (Ge) core the spectra are shown for the case without capping shells (solid lines), one (dotted lines), two (dashed lines), and three (dot-dashed lines) capping shells. The spectra are broadened by a Lorentzian width of 0.1 eV.

further the electron-hole pair energies in comparison to a Si NC with equal number of shells. This occurs because of the increasing size of the Si NC when capped with Ge and because of the increasing number of Ge atoms. On the other hand, the Si-capped Ge NCs show a compensation effect where their stoichiometry competes with the quantum confinement effects. At first glance, the addition of Si atom shells to the Ge core would increase the electron-hole pair energy of a NC if one considers only its composition. However, by adding Si shells the whole NC size is increased and the quantum confinement decreases, which leads to a reduction of the electron-hole pair energy. A similar decrease in the electron-hole pair excitation energies is predicted for Si NCs capped with Si oxide shells, a core-shell structure analogous to the Si-capped Ge NCs.[35,36]

In order to compare the confinement properties of the Si-(Ge-)capped Ge (Si) NCs to analogous Si/Ge heterostructures and capped II-VI NCs, we study the localization of the HOMOs and the LUMOs versus the distance from the center of the NC to its outermost shells. By means of an integration over the angles of the probability density distribution, one obtains the radial probability distributions $|\Psi(r)|^2$ of the HOMOs and the LUMOs shown in Fig. 6. The HOMO and LUMO radial probability distributions are compared to those of Si and Ge NCs. As a rule, both HOMO and LUMO are distributed in the whole extent of the capped NCs and Si (Ge) NCs. It is possible to recognize the shell structure of the NCs by means of the peaks in the radial probability distributions and this correspondence is more pronounced for the LUMOs of NCs with Ge core. In Fig. 6 one clearly sees that in the Ge-capped Si NCs the HOMO tends to localize more at the Ge outermost shells than in the Si core of the NC. In turn, the LUMOs remain mostly confined in the Si core without significant modifications with respect to the Si NCs of equivalent size. For the Si-capped Ge NCs the HOMOs have a similar distribution as for the Ge NCs, whereas the LUMO distribution mostly shifts toward the outermost Si shells. As a rule, the localization of electrons, identified with those of the LUMOs, and holes, identified with those of the HOMOs, follow what is generally expected for type-II planar Si/Ge heterostructures.[15,16] Also the localization of LUMOs and HOMOs in the Si-capped Ge NCs resembles the localization of HOMOs and LUMOs in CdS-capped CdSe NCs.[29] Since the electrons tend to be localized at the outermost Si shells, the Si-capped Ge NCs are expected to be very stable with respect to the photooxidation like in the case of CdS-capped CdSe NCs. Moreover, the presence of electrons in the outermost shells in principle make them more accessible, which is desirable for some optoelectronic applications.[29]

C. Optical absorption spectra

Optical absorption spectra of capped NCs are shown in Fig. 7 in comparison to the corresponding spectra of the Si and Ge NCs. As for the electron-hole pair excitation energies in Fig. 5, the increase of the size of the capped NCs and Si (Ge) NCs reduces the quantum confinement and tends to redshift both the onsets and the peaks of the absorption spectra. However, the magnitude of the shifts in the absorption spectra depends on the group-IV atoms in the core of the capped NCs. For Ge-capped Si NCs, the redshift of the absorption onset is much more pronounced than for the Si NCs with equal number of atoms. These effects on the absorption spectra can be explained essentially by quantum confinement effects, such as the NC size and the localization of electronic states, as well as by the increasing number of Ge atoms (cf. Fig. 4). On the other hand, for Si-capped Ge NCs one observes a compensation of quantum confinement effects besides the effect of the NC composition. An increasing number of Si atoms in the Si-capped Ge NCs tends to increase the value of the HOMO-LUMO gap, whereas the increasing size of the capped particles tends to reduce this value. As a

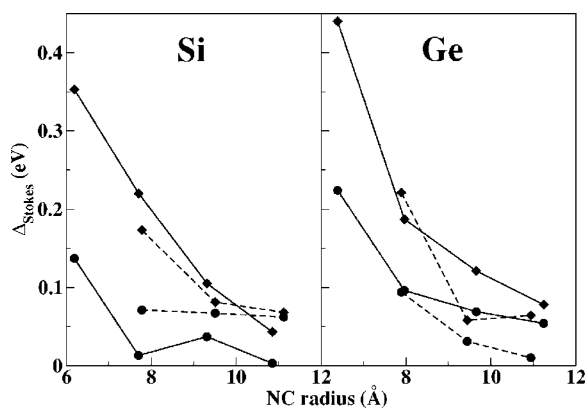

FIG. 8. Calculated Stokes shifts versus radius of the NC for the Si and Ge NCs (solid lines) and capped NCs (dashed lines). The values corresponding to ionic relaxations under the T_d-symmetry constraint (circles) and without symmetry constraint (diamonds) are shown.

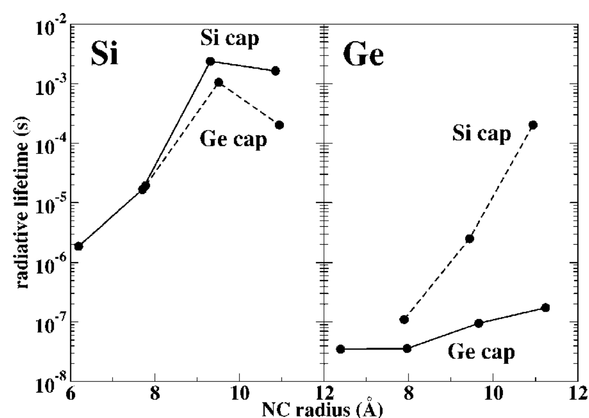

FIG. 9. Radiative lifetimes for the relaxed Si (left) and Ge (right) NCs versus NC radius at the temperature $T=300$ K. The dashed lines correspond to capped NCs and the solid lines to the Si and Ge NCs.

result, the redshift of the absorption onset and peaks for Si-capped Ge NCs is not as pronounced as in the case of Ge-capped Si NCs. In addition to this and more important are the changes in the localization of the electronic states, which in this case have more influence on the optical transition probabilities. As shown in Fig. 7, the changes in the optical transition probabilities affect differently the absorption spectra of Si-capped Ge NCs and Ge-capped Si NCs. Our predictions for the Si-capped Ge NCs are in agreement with the very small shifts in the absorption peaks measured for CdS-capped CdSe NCs with increasing number of capping shells.[29] Although the composition and the electronic properties of the CdS-capped CdSe NCs may be different, they have a localization of electrons and holes analogous to that of Si-capped Ge NCs.

D. Stokes shifts and radiative lifetimes

In the simplest picture, the excitation of an electron from the HOMO to the LUMO via photon absorption occurs in the ground-state geometry of the NC and creates an electron-hole pair. The system then relaxes and reaches the geometry configuration of the relaxed excited state with the lowest energy. For carrier lifetimes longer than the relaxation times, electrons and holes relax into their new electronic states accompanying the new geometry of the NC. Eventually the electron and hole may recombine and a photon emission occurs, this photon energy being usually smaller than the electron-hole pair excitation energies in Figs. 4 and 5. A measure of the energy loss due to ionic relaxation of capped NCs and Si (Ge) NCs is given by the Stokes shifts (Δ_{Stokes}) shown in Fig. 8. Although the values of the Stokes shifts are small in comparison to the pair excitation energies, they show how significantly the properties of Si NCs and Ge NCs can change due to few capping shells. In general, the Stokes shifts are larger for Ge NCs than for Si NCs passivated with H.[39] Figure 8 also shows the dependence of the Stokes shifts on the particular symmetry constraint used during the ionic relaxation. It is useful to consider both the case of T_d-symmetry constraint and the case of no symmetry constraint. Our calculations show that the total energies of the NCs in the ground state do not vary significantly when the constraint to T_d is removed and the system is left to relax under no symmetry constraint. On the other hand, for excited states the particular symmetry constraint is important and reduces the value of $E^*(N,e+h)$, consequently increasing the Stokes shifts of capped NCs and Si (Ge) NCs. The lack of symmetry constraint is more likely to correspond to the experiments, since the resulting electron density after a pair excitation may not be consistent with the symmetry of the ground state. In the case of NCs with a Si core, the trends of the Stokes shifts versus capping shells are different, according to the symmetry constraint for the ionic relaxation.[39,46] According to Fig. 8, the Stokes shifts calculated under the T_d-symmetry constraint are lower than the ones calculated under no symmetry constraint. This occurs because the lowering of the symmetry allows further rearrangement of the atoms and consequently increases the values of the Stokes shifts. The increase of the Stokes shifts also tends to be more pronounced in the NCs containing more Ge-Ge bonds, since these bonds are weaker than Si-Si bonds.

The radiative lifetimes (τ) calculated by Eq. (2) in the ground-state geometries are presented in Fig. 9. Differences in the radiative lifetimes of Si and Ge NCs can be understood in terms of the different Si-Si and Ge-Ge bond lengths and respective bonding energies. Because Ge has a smaller bonding energy than Si, the lattice deformation in the Ge regions of the NC is more drastic than in the Si regions. As a rule, the radiative lifetimes are more than two orders of magnitude larger for Si than for Ge NCs of same sizes. The Ge capping of Si NCs reduces the values of the radiative lifetimes by less than one order of magnitude, whereas the Si capping of Ge NCs is able to increase the lifetime values up to three orders of magnitude. For photodetection applications long radiative lifetimes are more important than large Stokes shifts, since the energy losses in the relaxation of the excited state are expected to be about ten times smaller than the photon energy. The longer radiative lifetimes of Ge-capped Si NCs and their relatively small changes with Ge capping make them

more suitable for photodetection than the Si-capped Ge NCs. On the other hand, the absorption onsets of Si-capped Ge NCs in Fig. 7 do not redshift remarkably with capping. For some applications that can keep nearly the same energy range of photon absorption, while increasing the radiative lifetimes to values comparable to the ones of Ge-capped Si NCs.

IV. CONCLUSIONS

We have presented first-principles investigations of Si-(Ge-)capped Ge (Si) NCs, their atomic structure, and electronic and optical properties. After ionic relaxation, the core-shell structure of the capped NCs can be clearly recognized by the distribution of the Si-Si and Ge-Ge bond lengths. These bond lengths even approach the ones of Si and Ge bulk in the case of the Si-capped Ge NCs. Si-capped Ge NCs have formation energies very similar to Ge NCs with the same number of atoms, whereas Ge-capped Si NCs are less stable in comparison to equivalent Si NCs. This explains why Si-capped Ge NCs are more common in growth experiments than their counterparts Ge-capped Si NCs. In both Si-capped Ge NCs and Ge-capped Si NCs the electrons tend to be more localized at the Si regions and the holes more localized at the Ge regions of the NC, resembling the localization of these carriers in analogous capped II-VI NCs and layered Si/Ge heterostructures. Although the capped NCs considered here are very well ordered in comparison to a SiGe-random-alloy NC, the electron-hole pair excitation energies versus composition follow the same trends as for random alloys. The electron-hole pair excitation energies and optical absorption spectra are much more affected by quantum confinement effects than by the stoichiometry of the capped NC. The increasing size of the capped NCs reduces quantum confinement and consequently reduces the values of electron-hole pair excitation energies and HOMO-LUMO gaps. Also the localization of electronic states more at the core or more at the capping shells plays an important role in the optical transitions. Depending on the group-IV species in the NC core (Si or Ge), the peaks in the absorption spectra have a different behavior with increasing number of capping shells. The absorption peaks of Si-capped Ge NCs redshift less than the corresponding peaks of Ge-capped Si NCs with equal number of shells, when the number of capping shells increases. Long radiative lifetimes in the Ge-capped Si NCs in principle favor them to photodetection applications, although comparable radiative lifetimes can be obtained with the Si capping of Ge NCs and without significant shifts of the absorption peaks.

ACKNOWLEDGMENTS

The authors are much obliged to the European Commission in the NANOQUANTA network of excellence (Contract No. NMP4-CT-2004-500198) and to the Fonds zur Förderung der Wissenschaftlichen Forschung (SFB 25, Austria 2005, "Nanostrukturen für Infrarot-Photonik") for financial support. The calculations were performed at the John von Neumann Institute for Computing (NIC) in Jülich, Germany (Grant No. HJN21/2004).

[1] D. L. Harame, S. J. Koester, G. Freeman, P. Cottrel, K. Rim, G. Dehlinger, D. Ahlgren, J. S. Dunn, D. Greenberg, A. Joseph, F. Anderson, J.-S. Rieh, S. A. S. T. Onge, D. Coolbaugh, V. Ramachandran, J. D. Cressler, and S. Subbanna, Appl. Surf. Sci. **224**, 9 (2004).
[2] B. Birtnar, Semicond. Sci. Technol. **18**, S221 (2003).
[3] C. W. Leitz, M. T. Currie, M. L. Lee, Z.-Y. Cheng, D. A. Antoniadis, and E. A. Fitzgerald, J. Appl. Phys. **92**, 3745 (2002).
[4] M. Jutzi and M. Berroth, in *Properties of Silicon Germanium and SiGe:Carbon*, edited by E. Kasper and K. Lyutovich, EMIS Data Review Series No. 24 (INSPEC, IEE, London, 2000), pp. 342–348.
[5] R. J. Zambrano, F. A. Rubinelli, W. M. Arnoldbik, J. K. Rath, and R. E. I. Schropp, Sol. Energy Mater. Sol. Cells **81**, 73 (2004).
[6] L. W. Teo, W. K. Choi, W. K. Chim, V. Ho, C. M. Moey, M. S. Tay, C. L. Heng, Y. Lei, D. A. Antoniadis, and E. A. Fitzgerald, Appl. Phys. Lett. **81**, 3639 (2002).
[7] H. G. Yang, Y. Shi, L. Pu, R. Zhang, B. Shen, P. Han, S. L. Gu, and Y. D. Zheng, Appl. Surf. Sci. **224**, 3 (2004).
[8] L. T. Canham, Appl. Phys. Lett. **57**, 1046 (1990).
[9] V. Lehmann and U. Gösele, Appl. Phys. Lett. **58**, 856 (1991).
[10] S. Bayliss, Q. Zhang, and P. Harris, Appl. Surf. Sci. **102**, 390 (1996).
[11] S. Furukawa and T. Miyasato, Phys. Rev. B **38**, 5726 (1988).
[12] Y. Maeda, Phys. Rev. B **51**, 1658 (1995).
[13] M. Zacharias and P. M. Fauchet, J. Non-Cryst. Solids **227-230**, 1058 (1998).
[14] L. Pavesi, L. Dal Negro, C. Mazzoleni, G. Franzó, and F. Priolo, Nature (London) **408**, 440 (2000).
[15] S. Ciraci and I. P. Batra, Phys. Rev. B **38**, 1835 (1988).
[16] K. B. Wong, M. Jaros, I. Morrison, and J. P. Hagon, Phys. Rev. Lett. **60**, 2221 (1988).
[17] E. Kasper and S. Heim, Appl. Surf. Sci. **224**, 3 (2004).
[18] C. Teichert, Phys. Rep. **365**, 335 (2002).
[19] Y.-W. Mo, D. E. Savage, B. S. Swartzentruber, and M. G. Lagally, Phys. Rev. Lett. **65**, 1020 (1990).
[20] D.-S. Lin, T. Miller, and T.-C. Chiang, Phys. Rev. B **47**, 6543 (1993).
[21] M. Stoffel, U. Denker, G. S. Kar, H. Sigg, and O. G. Schmidt, Appl. Phys. Lett. **83**, 2910 (2003).
[22] A. V. Kolobov, H. Oynagi, K. Brunner, G. Abstreiter, Y. Maeda, A. A. Shklyaev, S. Yamasaki, M. Ichikawa, and K. Tanaka, J. Vac. Sci. Technol. A **20**, 1116 (2002).
[23] Z. Zhong, J. Stangl, F. Schäffler, and G. Bauer, Appl. Phys. Lett. **83**, 3695 (2003).
[24] S. W. Lee, L. J. Chen, P. S. Chen, M.-J. Tsai, C. W. Liu, T. Y. Chien, and C. T. Chia, Appl. Phys. Lett. **83**, 5283 (2003).
[25] Y. Darma, R. Takaoka, H. Murakami, and S. Miyazaki, Nanotechnology **14**, 413 (2003).
[26] O. Kirfel, E. Müller, D. Grützmacher, K. Kern, A. Hesse, J.

Stangl, V. Holý, and G. Bauer, Appl. Surf. Sci. **224**, 139 (2004).

[27] A. Malachias, S. Kycia, G. Medeiros-Ribeiro, R. Magalhães-Paniago, T. I. Kamins, and R. S. Williams, Phys. Rev. Lett. **91**, 176101 (2003).

[28] M. A. Hines and P. Guyot-Sionnest, J. Phys. Chem. **100**, 468 (1996).

[29] X. Peng, M. C. Schlamp, A. V. Kadavanich, and A. P. Alivisatos, J. Am. Chem. Soc. **119**, 7019 (1997).

[30] V. I. Klimov, A. A. Mikhailovsku, S. Xu, A. Malko, J. A. Hollingsworth, C. A. Leatherdale, H.-J. Eisler, and M. G. Bawendi, Science **290**, 314 (2000).

[31] H. Hofmeister and P.Ködderitzsch, Nanostruct. Mater. **12**, 203 (1999).

[32] S. Öğüt, J. R. Chelikowsky, and S. G. Louie, Phys. Rev. Lett. **79**, 1770 (1997).

[33] L. X. Benedict, A. Puzder, A. J. Williamson, J. C. Grossman, G. Galli, J. E. Klepeis, J.-Y. Raty, and O. Pankratov, Phys. Rev. B **68**, 085310 (2003).

[34] E. Degoli, G. Cantele, E. Luppi, R. Magri, D. Ninno, O. Bisi, and S. Ossicini, Phys. Rev. B **69**, 155411 (2004).

[35] L. E. Ramos, J. Furthmüller, and F. Bechstedt, Phys. Rev. B **70**, 033311 (2004).

[36] L. E. Ramos, J. Furthmüller, and F. Bechstedt, Phys. Rev. B **71**, 035328 (2005).

[37] H.-Ch. Weissker, J. Furthmüller, and F. Bechstedt, Phys. Rev. Lett. **90**, 085501 (2003).

[38] H.-Ch. Weissker, J. Furthmüller, and F. Bechstedt, Phys. Rev. B **67**, 165322 (2003).

[39] H.-Ch. Weissker, J. Furthmüller, and F. Bechstedt, Phys. Rev. B **69**, 115310 (2004).

[40] J. D. Torre, N. Barriquand, M. D. Rouhani, and G. Landa, Eur. Phys. J. B **12**, 343 (1999).

[41] S. Balasubramanian, G. Ceder, and K. D. Kolenbrander, J. Appl. Phys. **79**, 4132 (1996).

[42] S.-F. Ren, W. Cheng, and P. Y. Yu, Phys. Rev. B **69**, 235327 (2004).

[43] G. Kresse and J. Furthmüller, Comput. Mater. Sci. **6**, 15 (1996).

[44] G. Kresse and J. Furthmüller, Phys. Rev. B **54**, 11169 (1996).

[45] G. Kresse and D. Joubert, Phys. Rev. B **59**, 1758 (1999).

[46] A. Franceschetti and S. T. Pantelides, Phys. Rev. B **68**, 033313 (2003).

[47] C. Delerue, G. Allan, and M. Lannoo, Phys. Rev. B **48**, 11024 (1993).

[48] G. Allan, C. Delerue, and Y. M. Niquet, Phys. Rev. B **63**, 205301 (2001).

[49] G. M. Dalpian, A. J. R. da Silva, and A. Fazzio, Phys. Rev. B **70**, 193306 (2004).

[50] J. C. Woicik, C. E. Bouldin, M. I. Bell, J. O. Cross, D. J. Tweet, B. D. Swanson, T. M. Zhang, L. B. Sorensen, C. A. King, J. L. Hoyt, P. Pianetta, and J. F. Gibbons, Phys. Rev. B **43**, 2419 (1991).

[51] P. Venezuela, G. M. Dalpian, A. J. R. da Silva, and A. Fazzio, Phys. Rev. B **64**, 193202 (2001).